Optik - International Journal for Light and Electron Optics 226 (2021) 165883

Contents lists available at ScienceDirect

Optik

journal homepage: www.elsevier.com/locate/ijleo

Original research article

On the performance of a novel multi-hop relay-assisted hybrid FSO / RF communication system with receive diversity

Mohammad Ali Amirabadi *, Vahid Tabataba Vakili

School of Electrical Engineering, Iran University of Science and Technology (IUST), Tehran, 1684613114, Iran

ARTICLE INFO

Keywords:
Free Space Optic / Radio Frequency
Gamma-Gamma
Negative exponential
Pointing error
Multi-hop
Receive diversity

ABSTRACT

One of the main problems in mobile communication systems is long-range links in weather conditions that could disrupt Radio Frequency (RF) connection. This problem could be solved by use of diversity or consuming more power or adding processing complexity. However, a mobile device has limited size and a small battery, and does not afford multiple antennas, or higher power consumption, or more complexity. So it is better to implement these techniques on the receiver, which is the base station. In this paper, a novel multi-hop hybrid Free Space Optical (FSO) / RF system is presented as a solution for the proposed scenario (long-range links in bad weather condition). In the proposed structure, a mobile user is connected to the source Base Station with receive diversity, and the source Base Station is connected to the destination Base Station via a multi-hop hybrid parallel FSO / RF link. In order to have a favorable performance with the lowest possible complexity, selection combining as well as demodulate and forward relaying are used at all hops of the proposed structure. The proposed structure has advantages of FSO, RF, and relay-assisted systems at the same time. The innovations and contributions of this paper, which are first introduced in the multi-hop hybrid FSO/ RF hybrid structure, include the novelty of the proposed structure, the presentation of new exact and asymptotic mathematical solutions, use of demodulate and forward protocol, taking into account a wide range of atmospheric turbulence with the effect of pointing error, use of selection combining at each relay. In order to show the efficiency of the proposed structure, Bit Error Rate and Outage Probability of the proposed structure are investigated in a wide range of atmospheric turbulence from moderate to saturate. Considering these criteria, closed-form exact and asymptotic expressions are derived and verified by MATLAB simulations. Results indicate that the proposed structure shows independent performance at moderate to strong atmospheric turbulence regimes. Hence, it is not required to adaptively adjust system parameters in order to have a constant performance. Accordingly, this structure is economically affordable and particularly suitable for mobile communications that should deal with frequent changes in atmospheric turbulence in urban by a limited complexity and power consumption.

1. Introduction

Intensity Modulation / Direct Detection (IM/DD) based on On-Off-Keying (OOK) has a simple implementation and is mostly used in Free Space Optical (FSO) Communication system [1]. The OOK requires channel estimation because its detection threshold is adjusted

* Corresponding author.
E-mail addresses: m_amirabadi@elec.iust.ac.ir (M.A. Amirabadi), vakily@iust.ac.ir (V. Tabataba Vakili).

https://doi.org/10.1016/j.ijleo.2020.165883
Received 17 May 2019; Received in revised form 19 May 2020; Accepted 23 October 2020
Available online 2 November 2020

based on the Channel State Information (CSI). Pulse Position Modulation (PPM) is another modulation format used in FSO system with lower spectral efficiency than OOK and fixed detection threshold. Subcarrier Intensity Modulation (SIM), due to its high spectral efficiency, is an appropriate alternative for both PPM and OOK but suffers from the carrier frequency and phase synchronization.

Terrestrial FSO link, due to easy and low-cost installation, license-free spectrum, high data rate, and security, is one of the main competitors of traditional Radio Frequency (RF) system. Performance of the FSO system is mainly affected by weather conditions, but even in clear weather, atmospheric turbulence caused by imbalance of temperature and pressure disrupts performance of the FSO link considerably. Scintillation, is one of the effects of atmospheric turbulence, which causes random fluctuations of the received signal intensity, and could be modeled by Log-Normal [2], Gamma-Gamma [3], K [4], I-K, H-K [5], M [6], and Negative Exponential [7] distributions. Among these models, Gamma-Gamma and Negative Exponential models have high accompany with experimental results obtained for moderate to strong and saturate regimes, respectively [8].

In addition to the atmospheric turbulence, misalignment of FSO transceiver, which is known as pointing error significantly degrades the performance of the FSO system. Based on vertical and horizontal displacements of the transceiver, this effect is divided into zero boresight and non-zero boresight effects. In zero boresight effect, horizontal and vertical displacements of incident light on the receiver plane are modeled by zero-mean Gaussian distribution, whereas in non-zero boresight effect, horizontal and vertical displacements are modeled by non-zero mean Gaussian distribution. In zero and non-zero boresight effects, radial displacements are modeled by Rayleigh and Rician distributions, respectively. Aperture averaging is a low-cost, simple and useful method to compensate mitigation caused by pointing error [9,10].

Practical applications of the FSO system are severely limited because of high sensitivity to atmospheric conditions as well as pointing error. Combining FSO and RF links improves system reliability, accessibility, capacity, and data rate [11]. Works done in the field of hybrid FSO / RF systems could be divided into three main categories. The first category considers the point-to-point FSO / RF system (single-hop structure) [10,12–21]. This category is composed of a parallel FSO / RF link, in which either both FSO and RF links are active, or FSO link is active and RF link acts as a back-up link [17,20]. It has worth to mention that the aim of this structure is improving reliability and data rate. Most of works done in this category considered a single user single input single out put link, however, few investigations considered multi-user [12] and receive diversity [18] scenarios [18] deployed different combining schemes such as Maximum Ratio Combiner, Equal Gain Combiner, and Selection Combiner in its proposed point-to-point FSO/RF system with receive diversity. The second category investigates dual-hop structure [22–48], which uses one relay station between source and destination, and improves capacity and reduces the total power consumption of the system. The dual-hop structure (the second category) could be divided into four sub-categories. The first sub-category considers a direct link (a back-up connection) between source and destination [22–31,49,50], and the second category does not consider this link [22,27–29,31–41,44–46,49]. The third sub-category considers single-user scenario [23,24,26,27,30,31,32–41,46], and the forth subcategory considers multi-user scenario [23,28,31,32,34,35,38,44,45,49]. The third category investigates multi-hop structure [21,51–55], which uses multiple relay stations between source and destination, and improves throughput of the system. This category has been investigated in the FSO system [51–53,56,57], but in hybrid FSO / RF system it is still a new topic [17,55,58–60]. These works implemented a single-user multi-hop hybrid parallel [55,58] or series [17,59,60] FSO / RF system.

Relay-assisted systems are known as a way of increasing the system capacity with low power requirements. The main difference between them is related to their processing, which is amplification [61] or decoding [41] or detection [62] the received signal and then forwarding it. Each of these schemes have their own advantages, therefore, according to consumer demands such as power, accuracy, timing, complexity, and cost, one of them can be used. Use of multi-hop relay-assisted structures in FSO systems improves data rate, capacity, and performance of the system. Various relaying schemes have been deployed in hybrid FSO / RF systems, including decode and forward [41], amplify and forward [40], quantize and forward [23]. Amplify and forward scheme amplifies the signal by either fixed or adaptive gain. The fixed gain scheme has less complexity but requires more power consumption, so, it is better to be used when CSI does not exist; when CSI exists, it is better to use the adaptive gain scheme [23]. Comparing with amplify and forward relaying, demodulate and forward has lower power consumption and does not enhance noise power. Therefore, in short-range links or long-range links that are divided into multiple hops, demodulate and forward is a better choice.

In the proposed structure in this paper a novel multi-hop relay-assisted hybrid FSO/RF system is presented. This structure is proposed as a solution for mobile communication in long-range links in bad weather conditions. Considering the battery and size limitations in mobile device, no additional processing is deployed on mobile station, and a source Base Station with receive diversity is used. Because of the fact that multi-hop relaying and parallel FSO / RF communicating are respectively efficient for long-range and bad weather conditions, the source Base Station is connected to the destination by a multi-hop hybrid parallel FSO / RF link. In order to have a complexity-performance trade-off, at all relay stations, selection combining (receive diversity [63]) with demodulate and forward relaying are used. The FSO link, at moderate to the strong regime, is described by Gamma-Gamma atmospheric turbulence with the effect of pointing error, and at saturate regime, is described by Negative Exponential atmospheric turbulence, and RF link has Rayleigh fading. Closed-form exact and asymptotic expressions are derived for Bit Error Rate (BER) and Outage Probability (P_{out}) of the proposed structure. MATLAB simulations are provided in order to validate the obtained results.

The remainder of this study is organized as follows: section II describes the system model. In sections III IV, and V, respectively P_{out}, BER, and diversity analysis of the proposed structure are discussed. Section VI provides simulation results and discussions and section VII is the conclusion of this work.

2. System model

The proposed structure of this paper is presented in Fig. 1. In this structure one mobile user transmits an RF signal, and the source

Base Station receives this signal via N receive antennas. The received signal with highest SNR is selected, and forwarded to the destination Base Station through a multi-hop hybrid FSO/RF link. Theoretical details of this transmission is provided in this section. Considering x, as the transmitted signal from the mobile user, the received signal at the first relay (source Base Station) becomes as follow:

$$y_{1,i} = h_{1,i}x + e_{1,i} \tag{1}$$

where, $e_{1,i}; i = 1, 2, \ldots, N$ is the Additive White Gaussian Noise (AWGN), with zero mean and σ^2_{RF} variance, at the first relay input, where N is number of receiving antennas, and h_i is the fading coefficient of path between user and $i-th$ receive antennas of the first relay.

Among received RF signals at the first relay, one with the highest SNR is selected, then demodulated, then regenerated, and then duplicated. One copy of the duplicated RF signal is converted to FSO signal by conversion efficiency of η and added by a unit amplitude DC bias (because FSO signal should be positive). The other copy of duplicated RF signal, plus the FSO signal are modulated and forwarded via a hybrid parallel FSO/RF link simultaneously. At all of the remaining relays, between received FSO and RF signals, one with higher SNR is selected, demodulated, regenerated and forwarded trough hybrid parallel FSO/RF link simultaneously. Actually, in hybrid FSO / RF links millimeter wave is used in RF link, because the FSO links support high data rate whereas the common RF links support comparative lower data rate. Accordingly, in each of the hybrid parallel FSO / RF links of the proposed system, data is encoded into parallel FSO and RF bits. Then the FSO link uses IM / DD while the RF link modulates the encoded bits and up converts the baseband signal into a millimeter wave with carrier frequency of 30−300 GHz.

This paper, in order to have a comprehensive investigation, and show the efficiency of the proposed structure, considers a wide range of atmospheric turbulence regimes from moderate to saturate. The best distributions for modeling these regimes are Gamma-Gamma for moderate to strong regimes and Negative Exponential for saturate regime. The probability density function (pdf) and Cumulative Distribution Function (CDF) of Gamma-Gamma distribution with the effect of pointing error [64], and the CDFs of Negative Exponential and Rayleigh distributions are respectively as follows:

$$f_\gamma(\gamma) = \frac{\xi^2}{2\Gamma(\alpha)\Gamma(\beta)\gamma} G^{3,0}_{1,4}\left(\alpha\beta\kappa\sqrt{\frac{\gamma}{\overline{\gamma}_{FSO}}}\ \begin{matrix}\xi^2+1\\ \xi^2,\alpha,\beta\end{matrix}\right) \tag{2}$$

$$F_\gamma(\gamma) = \frac{\xi^2}{\Gamma(\alpha)\Gamma(\beta)} G^{3,1}_{2,4}\left(\alpha\beta\kappa\sqrt{\frac{\gamma}{\overline{\gamma}_{FSO}}}\ \begin{matrix}1,\xi^2+1\\ \xi^2,\alpha,\beta,0\end{matrix}\right) \tag{3}$$

$$F_\gamma(\gamma) = 1 - e^{-\lambda\sqrt{\frac{\gamma}{\overline{\gamma}_{FSO}}}} \tag{4}$$

$$F_\gamma(\gamma) = 1 - e^{-\frac{\gamma}{\overline{\gamma}_{RF}}} \tag{5}$$

where $G^{-}_{-}\left(\begin{matrix}-\\-\end{matrix}\right)$ is the Meijer-G function [65], α, β and ξ are characterization parameters of Gamma-Gamma atmospheric turbulence, and pointing error, respectively [64], and $\Gamma()$ is Gamma function [65]. $\overline{\gamma}_{FSO} = E[x^2]\eta^2/\sigma^2_{FSO}$ and $\overline{\gamma}_{RF} = E[x^2]/\sigma^2_{RF}$ are the average SNR at FSO and RF receiver inputs, respectively, and σ^2_{FSO} and σ^2_{RF} are AWGN variances at FSO and RF receiver inputs.

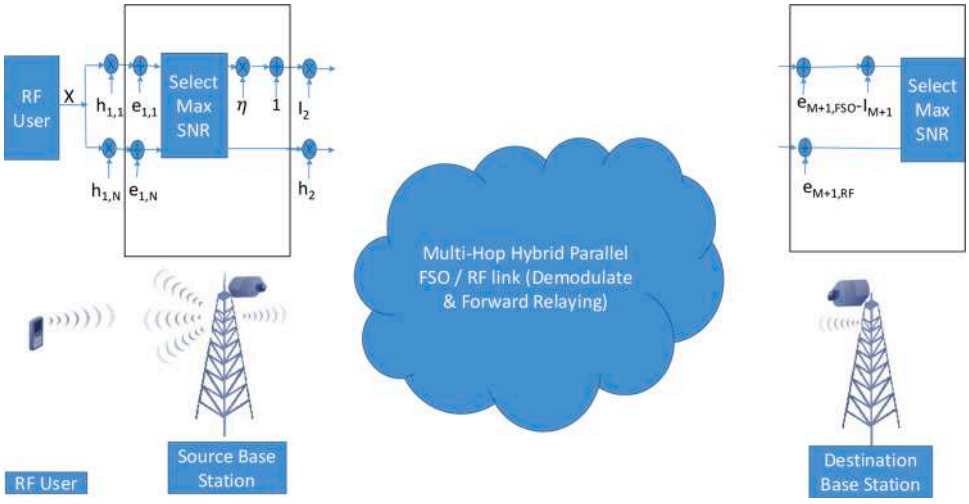

Fig. 1. The proposed multi-hop relay-assisted hybrid FSO / RF system with receive diversity.

According that the first relay selects signal with the highest SNR, and the RF links are independent and identically distributed, the CDF of instantaneous SNR at the first relay input (γ_1) becomes as follow:

$$F_{\gamma_1}(\gamma)=\Pr\left(\max\left(\gamma_{1,1},\gamma_{1,2},\ldots,\gamma_{1,N}\right)\le\gamma\right)=\Pr\left(\gamma_{1,1}\le\gamma,\gamma_{1,2}\le\gamma,\ldots,\gamma_{1,N}\le\gamma\right)=\prod_{i=1}^{N}\Pr\left(\gamma_{1,i}\le\gamma\right)=\prod_{i=1}^{N}F_{\gamma_{1,i}}(\gamma)=\left(1-e^{-\frac{\gamma}{\bar{\gamma}_{RF}}}\right)^{N}. \tag{6}$$

Between received FSO and RF signals at $j-th;j=2,3,\ldots M$ relay (is the number of relays), one with higher SNR is selected; therefore, the CDF of instantaneous SNR at the $j-th$ relay input (γ_j) becomes equal to:

$$F_{\gamma_j}(\gamma)=\Pr\left(\max\left(\gamma_{j,1},\gamma_{j,2}\right)\le\gamma\right)=\Pr\left(\gamma_{j,1}\le\gamma,\gamma_{j,2}\le\gamma\right)=F_{\gamma_{j,1}}(\gamma)F_{\gamma_{j,2}}(\gamma) \tag{7}$$

The last equality is because of the independence of FSO and RF links.

3. Outage probability

In the proposed structure, an outage occurs while the SNR of the received signal at each of the relay stations comes down below a threshold level. The link availability of a multi-hop structure is equal to the multiplication of link availabilities of each of individual hops [59]. Therefore, P_{out} of the proposed structure becomes equal to:

$$\begin{aligned}P_{out}(\gamma_{th})&=\Pr\{(\gamma_1,\gamma_2,\ldots,\gamma_{M+1})\le\gamma_{th}\}=1-\Pr\{\gamma_1\ge\gamma_{th},\gamma_2\ge\gamma_{th},\ldots,\gamma_{M+1}\ge\gamma_{th}\}=1-(1-\Pr\{(\gamma_1\le\gamma_{th})\})\,(1-\Pr\{(\gamma_2\\&\le\gamma_{th})\})\,(1-\Pr\{(\gamma_{M+1}\le\gamma_{th})\})\;=1-(1-\mathrm{F}_{\gamma_1}(\gamma_{\mathrm{th}}))(1-\mathrm{F}_{\gamma_2}(\gamma_{\mathrm{th}}))\ldots(1-\mathrm{F}_{\gamma_{M+1}}(\gamma_{\mathrm{th}}))\end{aligned} \tag{8}$$

Except for the first link, the other links have the same structure; therefore, P_{out} of the proposed structure becomes equal to:

$$P_{out}(\gamma_{th})=1-(1-F_{\gamma_1}(\gamma_{th}))\left(1-F_{\gamma_j}(\gamma_{th})\right)^{M} \tag{9}$$

Considering (7), and by substituting (3), (5) and (6) into (9), P_{out} of the proposed structure in Gamma-Gamma atmospheric turbulence with the effect of pointing error becomes as follows:

$$P_{out}(\gamma_{th})=1-\left(1-\left(1-e^{-\frac{\gamma_{th}}{\bar{\gamma}_{RF}}}\right)^{N}\right)\left(1-\frac{\xi^2}{\Gamma(\alpha)\Gamma(\beta)}\left(1-e^{-\frac{\gamma_{th}}{\bar{\gamma}_{RF}}}\right)G_{2,4}^{3,1}\left(\alpha\beta\kappa\sqrt{\frac{\gamma_{th}}{\bar{\gamma}_{FSO}}}\;\begin{matrix}1,\xi^2+1\\ \xi^2,\alpha,\beta,0\end{matrix}\right)\right)^{M}. \tag{10}$$

In the derivation of BER in section IV, (10) will be used, but it's somehow complex and needs to be simplified more. By substituting binomial expansion of $\left(1-e^{-\frac{\gamma_{th}}{\bar{\gamma}_{RF}}}\right)^{N}$ and $\left(1-\frac{\xi^2}{\Gamma(\alpha)\Gamma(\beta)}\left(1-e^{-\frac{\gamma_{th}}{\bar{\gamma}_{RF}}}\right)\times G_{2,4}^{3,1}\left(\alpha\beta\kappa\sqrt{\frac{\gamma_{th}}{\bar{\gamma}_{FSO}}}\;\begin{matrix}1,\xi^2+1\\ \xi^2,\alpha,\beta,0\end{matrix}\right)\right)^{M}$, P_{out} of the proposed structure in Gamma-Gamma atmospheric turbulence with the effect of pointing error is as follows:

$$P_{out}(\gamma_{th})=1+\sum_{k=1}^{N}\sum_{t=0}^{M}\sum_{u=0}^{t}\Omega e^{-\frac{(k+u)\gamma_{th}}{\bar{\gamma}_{RF}}}\left(\frac{\xi^2}{\Gamma(\alpha)\Gamma(\beta)}G_{2,4}^{3,1}\left(\alpha\beta\kappa\sqrt{\frac{\gamma_{th}}{\bar{\gamma}_{FSO}}}\;\begin{matrix}1,\xi^2+1\\ \xi^2,\alpha,\;\beta,0\end{matrix}\right)\right)^{t}, \tag{11}$$

where $\Omega=\binom{N}{k}\binom{M}{t}\binom{t}{u}(-1)^{k+t+u}$. As can be seen, the weight of the CDF of RF link in the above expression is more and it's something logical because there RF links are more than FSO links.

According to (7), and by substituting (4), (5) and (6) into (9), P_{out} of the proposed structure in Negative Exponential atmospheric turbulence becomes as follows:

$$P_{out}(\gamma_{th})=1-\left(1-\left(1-e^{-\frac{\gamma_{th}}{\bar{\gamma}_{RF}}}\right)^{N}\right)\left(1-\left(1-e^{-\frac{\gamma_{th}}{\bar{\gamma}_{RF}}}\right)\left(1-e^{-\lambda\sqrt{\frac{\gamma_{th}}{\bar{\gamma}_{FSO}}}}\right)\right)^{M}. \tag{12}$$

By substituting binomial expansions of $\left(1-e^{\frac{\gamma_{th}}{\bar{\gamma}_{RF}}}\right)^{N}$ and $\left(1-\left(1-e^{-\frac{\gamma_{th}}{\bar{\gamma}_{RF}}}\right)\left(1-e^{-\lambda\sqrt{\frac{\gamma_{th}}{\bar{\gamma}_{FSO}}}}\right)\right)^{M}$, P_{out} of the proposed structure in Negative Exponential atmospheric turbulence becomes as follow:

$$P_{out}(\gamma_{th})=1+\sum_{k=1}^{N}\sum_{t=0}^{M}\sum_{u=0}^{t}\sum_{v=0}^{t}\Lambda e^{-\frac{(k+u)\gamma_{th}}{\bar{\gamma}_{RF}}}e^{-\lambda v\sqrt{\frac{\gamma_{th}}{\bar{\gamma}_{FSO}}}}, \tag{13}$$

where $\Lambda=\binom{N}{k}\binom{M}{t}\binom{t}{u}\binom{t}{v}(-1)^{k+t+u+v}$. Although there are 3 and 4 summations in (11) and (13), respectively, it should be considered that this complexity is because of assuming a complex structure.

4. Bit error rate

In this paper DPSK modulation is used, differential modulations such as DPSK, are less sensitive to noise and interference, and because of the following reasons, their detection is optimal: no need for CSI or complex processing at the receiver, no need for threshold adjustment feedback, no effect on system throughput due to lack of pilot or training sequence, reduction in the effects of background noise at the receiver, reduction in effects of pointing error and weather conditions such as fog and mist. BER of DPSK modulation is calculated from the following expression [11]:

$$P_e = \frac{1}{2}\int_0^\infty e^{-\gamma}F_\gamma(\gamma)d\gamma = \frac{1}{2}\int_0^\infty e^{-\gamma}P_{out}(\gamma)d\gamma. \tag{14}$$

The last inequality appeared because *of* $F_\gamma(\gamma) = P_{out}(\gamma)$. BER of DPSK modulation in Gamma-Gamma atmospheric turbulence with the effect of pointing error can be obtained by substituting (11) into (14):

$$P_e = \frac{1}{2}\int_0^\infty e^{-\gamma}\left\{1+\sum_{k=1}^{N}\sum_{t=0}^{M}\sum_{u=0}^{t}\Omega e^{-\frac{(k+u)\gamma}{\overline{\gamma}_{RF}}}\left(\frac{\xi^2}{\Gamma(\alpha)\Gamma(\beta)}G_{2,4}^{3,1}\left(\alpha\beta\kappa\sqrt{\frac{\gamma}{\overline{\gamma}_{FSO}}}\ \begin{matrix}1,\xi^2+1\\ \xi^2,\alpha,\ \beta,0\end{matrix}\right)\right)^t\right\}d\gamma. \tag{15}$$

When $t > 2$, because of the multiplication of three Meijer-G and one exponential functions, the above integral cannot be solved. This paper tries to solve this problem and derives asymptotic and exact expressions in closed-form for BER and outage probability of the proposed structure in Gamma-Gamma atmospheric turbulence with the effect of pointing error.

4.1. Exact BER for Gamma-Gamma atmospheric turbulence with the effect on pointing error

By substituting exact equivalent of the CDF of Gamma-Gamma atmospheric turbulence with the effect of pointing error from Appendix A into (11), and by substituting binomial expansion of $\left(X_0\left(\frac{\gamma_{th}}{\overline{\gamma}_{FSO}}\right)^{\frac{\xi^2}{2}}+\sum_{n=0}^{\infty}Y_n\left(\frac{\gamma_{th}}{\overline{\gamma}_{FSO}}\right)^{\frac{n+\alpha}{2}}+\sum_{n=0}^{\infty}Z_n\left(\frac{\gamma_{th}}{\overline{\gamma}_{FSO}}\right)^{\frac{n+\beta}{2}}\right)^t$ as $\sum_{k_1=0}^{t}\sum_{k_2=0}^{k_1}\binom{t}{k_1}\binom{k_1}{k_2}\left(X_0\left(\frac{\gamma_{th}}{\overline{\gamma}_{FSO}}\right)^{\frac{\xi^2}{2}}\right)^{t-k_1}\left(\sum_{n=0}^{\infty}Y_n\left(\frac{\gamma_{th}}{\overline{\gamma}_{FSO}}\right)^{\frac{n+\alpha}{2}}\right)^{k_1-k_2}\times\left(\sum_{n=0}^{\infty}Z_n\left(\frac{\gamma_{th}}{\overline{\gamma}_{FSO}}\right)^{\frac{n+\beta}{2}}\right)^{k_2}$ and a bit mathematical simplification, P_{out} of the proposed structure in Gamma-Gamma atmospheric turbulence with the effect of pointing error becomes equal to:

$$P_{out}(\gamma_{th}) = 1+\sum_{k=1}^{N}\sum_{t=0}^{M}\sum_{u=0}^{t}\sum_{k_1=0}^{t}\sum_{k_2=0}^{k_1}\sum_{n=0}^{\infty}\Omega\binom{t}{k_1}\binom{k_1}{k_2}X_0^{t-k_1}\left(Y_n^{(k_1-k_2)}*Z_n^{(k_2)}\right)e^{-\frac{(k+u)\gamma_{th}}{\overline{\gamma}_{RF}}}\left(\frac{\gamma_{th}}{\overline{\gamma}_{FSO}}\right)^{\frac{n+\xi^2(t-k_1)+\alpha(k_1-k_2)+\beta k_2}{2}}. \tag{16}$$

By substituting (16) into (14), BER of DPSK modulation in Gamma-Gamma atmospheric turbulence with the effect of pointing error becomes equal to:

$$P_e = \frac{1}{2}\left\{1+\sum_{k=1}^{N}\sum_{t=0}^{M}\sum_{u=0}^{t}\sum_{k_1=0}^{t}\sum_{k_2=0}^{k_1}\sum_{n=0}^{\infty}\Omega\binom{t}{k_1}\binom{k_1}{k_2}X_0^{t-k_1}\left(Y_n^{(k_1-k_2)}*Z_n^{(k_2)}\right)\frac{\left(1/\overline{\gamma}_{FSO}\right)^{\frac{n+\xi^2(t-k_1)+\alpha(k_1-k_2)+\beta k_2}{2}}}{\left(1+\frac{k+u}{\overline{\gamma}_{RF}}\right)^{1+\frac{n+\xi^2(t-k_1)+\alpha(k_1-k_2)+\beta k_2}{2}}}\right\} \tag{17}$$

It is evident from (16) and (17) that the number of antennas and number of relays have impact on the performance of the proposed structure, but it could be interesting to know which one is more important. This is investigated in the results section.

4.2. Asymptotic BER of Gamma-Gamma atmospheric turbulence with the effect of pointing error

According to the complexity of (16) and (17), it's not easy to have enough insights about them; therefore, deriving some asymptotic expressions could help to get some more analytical insights about the performance of the proposed structure. By substituting the CDF of Gamma-Gamma atmospheric turbulence with the effect of pointing error, from Appendix B into (11), P_{out} of the proposed system becomes as follows:

$$P_{out}(\gamma_{th}) \cong \begin{cases} 1+\sum_{k=1}^{N}\sum_{t=0}^{M}\sum_{u=0}^{t} e^{-\frac{(k+u)\gamma_{th}}{\overline{\gamma}_{RF}}}\Omega(\varpi)^t\gamma_{th}^{\frac{\beta t}{2}} & (1) \\ 1+\sum_{k=1}^{N}\sum_{t=0}^{M}\sum_{u=0}^{t} e^{-\frac{(k+u)\gamma_{th}}{\overline{\gamma}_{RF}}}\Omega(\rho)^t\gamma_{th}^{\frac{\xi^2 t}{2}} & (2) \\ 1+\sum_{k=1}^{N}\sum_{t=0}^{M}\sum_{u=0}^{t} e^{-\frac{(k+u)\gamma_{th}}{\overline{\gamma}_{RF}}}\Omega(\vartheta)^t\gamma_{th}^{\frac{\alpha t}{2}} & (3) \end{cases} \tag{18}$$

As can be seen (18) is a simple linear equation. It is very easy to have enough insights into it. In statement $\exp(-(k+u)\gamma_{th}/\overline{\gamma}_{RF})$, the component k (which is upper bounded by N) is at the exponent multiplied by a minus sign; therefore, P_{out} decreases by increasing number of receive antennas (N). In serial relay structures, it is expected that the increasing number of relays increases P_{out} because an increasing number of relays increases the number of decisions made on the signal and leads to increase of the outage probability. In (18), the component t (which is related to M), is on the power of γ_{th}, increasing this component increases the P_{out}. By substituting the (18) into (15), the asymptotic BER of DPSK modulation in Gamma-Gamma atmospheric turbulence with the effect of pointing error becomes equal to:

$$P_e \cong \begin{cases} 1+\sum_{k=1}^{N}\sum_{t=0}^{M}\sum_{u=0}^{t}\dfrac{\Omega(\varpi)^t\Gamma\left(\frac{\beta t}{2}+1\right)}{\left(1+\frac{k+u}{\overline{\gamma}_{RF}}\right)^{\frac{\beta t}{2}+1}} & (1) \\ 1+\sum_{k=1}^{N}\sum_{t=0}^{M}\sum_{u=0}^{t}\dfrac{\Omega(\rho)^t\Gamma\left(\frac{\xi^2 t}{2}+1\right)}{\left(1+\frac{k+u}{\overline{\gamma}_{RF}}\right)^{\frac{\xi^2 t}{2}+1}} & (2) \\ 1+\sum_{k=1}^{N}\sum_{t=0}^{M}\sum_{u=0}^{t}\dfrac{\Omega(\vartheta)^t\Gamma\left(\frac{\alpha t}{2}+1\right)}{\left(1+\frac{k+u}{\overline{\gamma}_{RF}}\right)^{\frac{\alpha t}{2}+1}} & (3) \end{cases} \tag{19}$$

The same as (18), (19) is a simple linear function the same insights as (18) could be stated for it. Substituting (13) into (14), and substituting Meijer-G equivalent of $e^{-\lambda v\sqrt{\frac{\gamma}{\overline{\gamma}_{FSO}}}}$ as $\frac{1}{\sqrt{\pi}}G_{0,2}^{2,0}\left(\frac{(\lambda v)^2\gamma}{4\overline{\gamma}_{FSO}}\ \begin{matrix}-\\ 0,0.5\end{matrix}\right)$ and using [63], BER of DPSK modulation in Negative Exponential atmospheric turbulence becomes equal to:

$$P_e = \frac{1}{2}\left\{\sum_{k=1}^{N}\sum_{t=0}^{M}\sum_{u=0}^{t}\sum_{v=0}^{t}\Lambda\frac{1}{\sqrt{\pi}}\frac{1}{1+\frac{k+u}{\overline{\gamma}_{RF}}}\times G_{1,2}^{2,1}\left(\frac{(\lambda v)^2}{4\overline{\gamma}_{FSO}\left(1+\frac{k+u}{\overline{\gamma}_{RF}}\right)}\ \begin{matrix}0\\ 0,0.5\end{matrix}\right)\right\} \tag{20}$$

Although with modern computing tools, it is now easier to produce analytical expressions, even modern computing tools cannot get forms shorter than the derived formulations. Because these expressions are in the form of Meijer-G function, which is the shortest possible equivalent for mathematical expressions. The Meijer-G is a mathematical tool used in literature without significant insights.

Although the mathematical formulations are a bit complex, it's not necessary to challenge in the mathematical area; while plotting these expressions, could easily have useful insights. The complexity of derived expressions is related to 1) using Meijer-G function, which has complex structure by itself, and 2) the inherent complexity of the proposed structure.

5. Diversity

Diversity gain is the increase in SNR because of a diversity scheme, or how much the γ_{avg} could be reduced when a diversity scheme is introduced, without a performance loss. It is usually expressed in decibels; when plotting the P_{out} versus γ_{avg}, it could be observed as the tangent of the plotted figure at high γ_{avg}. Considering the first hop, the selection of the strongest signal between N received signals in Rayleigh i.i.d. distribution, the expected diversity gain has been shown to be $\sum_{k=1}^{N}1/k$. However, the addition of serial hops after the first hop reduces the diversity gain. The diversity is dominated by the smallest exponent of the γ_{avg}. At high γ_{avg}, P_{out} can be represented as [46,55]

$$P_{out}^{\infty}(\gamma_{th}) = G_c\gamma_{avg}^{-G_d} \tag{21}$$

For finding the diversity order of the proposed structure in Gamma-Gamma atmospheric turbulence with the effect of pointing error

(16) should be considered (because it includes only finite summations of elementary functions) and the following minimization problem should be solved:

$$\min \frac{2k + 3n + \xi^2(t - k_1) + \alpha(k_1 - k_2) + \beta k_2}{2} \tag{22}$$

Considering the range of $k, n, t, k_1,$ *and* k_2, the solution of the above minimization is $G_d = 1$; this is also indicated in simulation results, where for different scenarios, at high SNRs the tangent of the P_{out} curves are parallel with unit tangent. For finding the diversity order of the proposed structure in Negative Exponential atmospheric turbulence (13) should be considered (because it includes only finite summations of elementary functions) and the following minimization problem should be solved:

$$\min \frac{2k + 3n}{2} \tag{23}$$

Considering the range of k, and n the solution of the above minimization is $G_d = 1$; this is also indicated in simulation results, where for different scenarios, at high SNRs the tangent of the P_{out} curves are parallel with unit tangent.

6. Comparison of simulation and analytical results

In this section, MATLAB simulation and analytical results of the performance of the proposed structure are compared and discussed. Without loss of generality, it is assumed that FSO and RF links have the same average SNR ($\gamma_{avg} = \overline{\gamma}_{FSO} = \overline{\gamma}_{RF}$) and $\eta = 1$. The proposed structure is investigated at various number of receive antennas (N) and relays (M), and at different atmospheric turbulence regimes, from moderate to saturate. The outage threshold SNR is denoted by γ_{th}.

In Fig. 2, Outage Probability of the proposed structure is plotted as a function of average SNR for various number of receive antennas for Negative Exponential atmospheric turbulence with unit variance, when number of relays is $M = 2$ and $\gamma_{th} = 10dB$. As can be seen, performance of the proposed structure has low dependence on the number of receive antennas. Generally, a system with multiple receive antennas performs better than a system with a single receive antenna. The proposed structure uses selection combiner and therefore, by an increase in the number of receive antenna, it is more likely that the SNR of the selected signal is higher than the threshold level.

In Fig. 3, Outage Probability of the proposed structure is plotted as a function of average SNR for various number of relays for Negative Exponential atmospheric turbulence with unit variance, when number of receive antennas is $N = 2$ and $\gamma_{th} = 10dB$. At $P_{out} = 10^{-4}$, γ_{avg} difference between system performance at $M = 1$ and $M = 2, 3, 4$, is about $2dB$, 3 dB and 4 dB, respectively. At a wide range of target P_{out}, the same γ_{avg} difference values can be observed. In series relay structure, performance degrades by relay addition. However, because γ_{avg} difference values at different target P_{out} are the same, only constant fraction of consumed power should be added to compensate this degradation, and it is not required additional processing to adjust this fraction adaptively.

In Fig. 4, Outage Probability of the proposed structure is plotted as a function of average SNR for various variances of Negative Exponential atmospheric turbulence when the number of receive antennas is $N = 2$, the number of relays is $M = 2$ and $\gamma_{th} = 10dB$. It can be seen that the proposed structure is severely dependent on atmospheric turbulence variance; for example, at $P_{out} = 10^{-3}$, γ_{avg} difference between system performance of the cases of $\lambda = 1$ and $\lambda = 2$, also between the cases of $\lambda = 1$ and $\lambda = 5$, is about $2dB$ and $5dB$, respectively. This difference changes at different target P_{out}, thereby, the proposed structure is not recommended for non-urban cells with high changes in atmospheric turbulence. But generally speaking at these places, because of the dependence on atmospheric turbulence, much more power is required to compensate for the degradation caused by atmospheric turbulence.

In Fig. 5, Bit Error Rate of the proposed structure is plotted as a function of average SNR for moderate ($\alpha = 4, \beta = 1.9, \xi = 10.45$) and strong ($\alpha = 4.2, \beta = 1.4, \xi = 2.45$), regimes of Gamma-Gamma atmospheric turbulence with the effect of pointing error, when

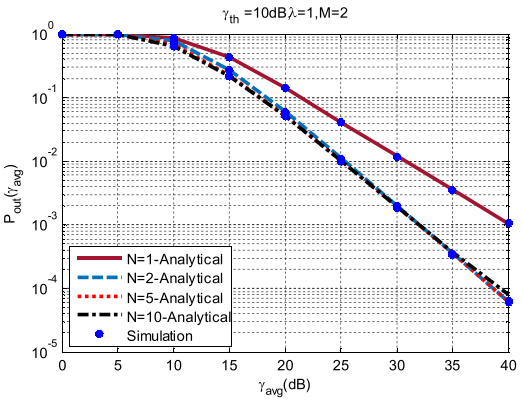

Fig. 2. Outage Probability of the proposed structure as a function of average SNR for various number of receive antennas for Negative Exponential atmospheric turbulence with unit variance, when number of relays is $M = 2$ and $\gamma_{th} = 10dB$.

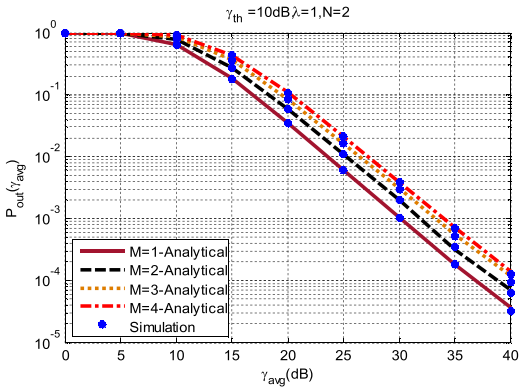

Fig. 3. Outage Probability of the proposed structure as a function of average SNR for various number of relays for Negative Exponential atmospheric turbulence with unit variance, when the number of receive antennas is $N = 2$ and $\gamma_{th} = 10dB$.

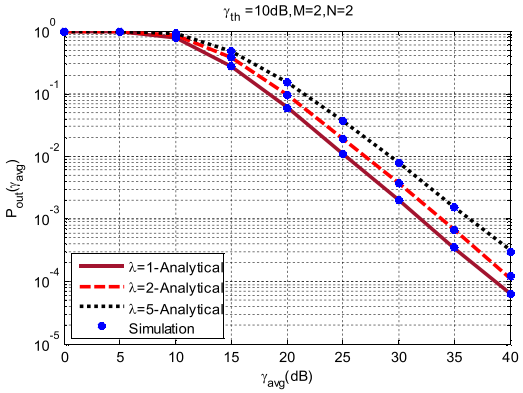

Fig. 4. Outage Probability of the proposed structure as a function of average SNR for various variances of Negative Exponential atmospheric turbulence, when number of receive antennas is $N = 2$, number of relays is $M = 2$ and $\gamma_{th} = 10dB$.

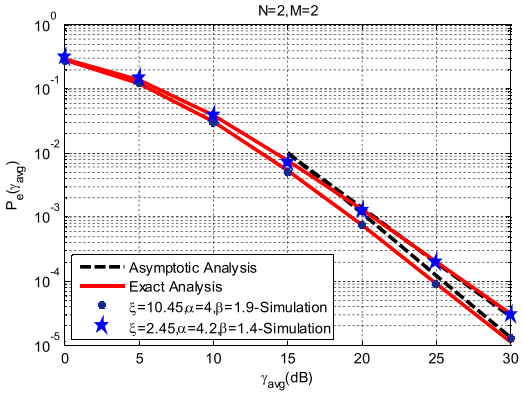

Fig. 5. Bit Error Rate of the proposed structure as a function of average SNR for moderate ($\alpha = 4, \beta = 1.9, \xi = 10.45$) and strong ($\alpha = 4.2, \beta = 1.4$, $\xi = 2.45$), regimes of Gamma-Gamma atmospheric turbulence with the effect of pointing error, when the number of receive antennas is $N = 2$ and number of relays is $M = 2$.

number of receive antenna is $N = 2$ and the number of relays is $M = 2$. It can be seen that there is little γ_{avg} difference between system performance at moderate and strong atmospheric turbulence regimes, for example, at $P_e = 10^{-4}$ and $P_e = 10^{-3}$, this difference is about $1.5dB$ and $2dB$, respectively. Therefore, this structure is suitable for urban cells which encounter with frequent changes in atmospheric turbulence. This structure is not sensitive to changes in atmospheric turbulence, therefore it does not need an adaptive processor in order to maintain performance. From this point of view, it has less complexity and installation cost.

In Fig. 6, Outage Probability of the proposed structure is plotted as a function of average SNR for various number of relays for moderate ($\alpha = 4, \beta = 1.9, \xi = 10.45$) regime of Gamma-Gamma atmospheric turbulence with the effects of pointing error when the number of antennas is $N = 2$ and $\gamma_{th} = 10dB$. It can be seen that at $P_{out} = 10^{-4}$, the γ_{avg} difference between system performance at the case of $M = 1$ and cases of $M = 2, 3, 4$ are about 1.5 dB, 2 dB, and 3 dB, respectively. Of course, the degradation caused by relay addition is compensable by consuming power, therefore the proposed structure is particularly suitable for communication cells which service huge number of users.

In Fig. 7, Outage probability of the proposed structure is plotted as a function of average SNR for different number of receive antennas, for the moderate regime of Gamma-Gamma atmospheric turbulence with the effect of pointing error, when the number of relays is $M = 2$ and $\gamma_{th} = 10dB$. As can be seen, the proposed structure has little dependence on the number of receive antennas. This is due to the selection of the antenna with the highest SNR. Since different received signal encounter with independent fading, with the increase in the number of antennas, it is more likely to find the signal with favorable SNR level.

Fig. 8 plots Bit Error Rate of the proposed structure as a function of average SNR for different number of transmitter antennas, for moderate ($\alpha = 4, \beta = 1.9, \xi = 10.45$) regime of Gamma-Gamma atmospheric turbulence with the effect of pointing error, when number of relays is $M = 2$. As could be seen, increasing number of receive antennas improves the performance, however, due to the fact that the effect of the first hop on the performance is lower than other hops, increasing number of antennas does not improve performance continuously, and as could be seen, $N = 2$ has much better performance than $N = 1$, but $N = 5$ does not have much better performance than $N = 2$. It should be noted that the performance of a multi-hop system is dependent on all of its hops and not just one hop. So, it is not expected that increasing complexity and processing in one hop yields to performance improvement in the whole system (which is exactly seen in this figure).

Fig. 9 plots Bit Error Rate of the proposed structure as a function of average SNR for various variances of Negative Exponential atmospheric turbulence, when number of receive antennas is $N = 2$ and number of relays is $M = 2$. As could be seen, the proposed structure has a favorable performance even at different variances of the Negative Exponential atmospheric turbulence. At low SNRs, which the noise effect is dominant, system has the same performance at different variances of the Negative Exponential atmospheric turbulence, and the difference appears while increasing the SNR. However, at high SNRs the same diversity gain is observable for different scenarios, which is as expected while deriving the diversity gain formula. This is actually one the benefits of the proposed structure, because it brings the same diversity gain at different scenarios, it could be trustable for applying at links with varying conditions, for example in Mediterranean links, which atmospheric turbulence changes during the day.

Fig. 10 plots Bit Error Rate of the proposed structure as a function of average SNR for different number of receive antennas and different number of relays, for Negative Exponential atmospheric turbulence with unit variance. This figure looks at the problem from another view, it says that although increasing number of antennas improves the performance, however, the effect of addition number of hops on performance degradation is more observable. As could be seen $N = 3 = M = 3$ has worse performance than $N = 2$, $M = 2$. The same statements as other figures exists here about the diversity gain and having favorable performance at different SNRs.

7. Conclusion

In this study, a novel multi-hop relay-assisted hybrid FSO / RF structure was presented, in which a mobile user was connected to the source Base Station via an RF link with receive diversity, source and destination Base Stations were connected via a multi-hop hybrid FSO / RF link. Demodulate and forward protocol was used in this multi-hop structure. At each link, the signal with higher SNR was selected for transmission. The effects of the number of receive antennas as well as the number of relays on the performance of the proposed structure were investigated at various atmospheric turbulence form moderate to saturate regimes. Changing the number of receive antennas did not affect the performance so much. Also, the performance difference between different numbers of relays was almost constant; therefore, it does not require adaptive processing in order to define the fraction of additional power for maintaining system performance. Hence the proposed structure increases capacity while maintaining the performance of the system, with low

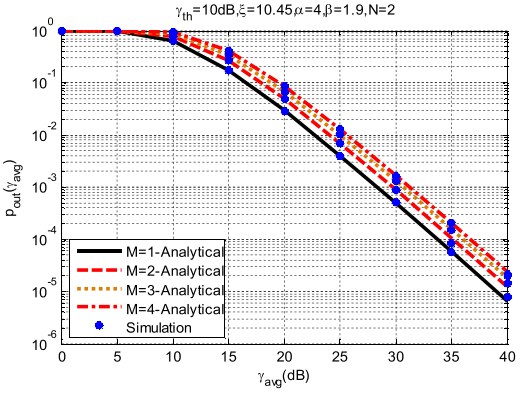

Fig. 6. Outage probability of the proposed structure as a function of average SNR for various number of relays for moderate ($\alpha = 4, \beta = 1.9, \xi = 10.45$) regime of Gamma-Gamma atmospheric turbulence with the effects of pointing error, when the number of antennas is $N = 2$ and $\gamma_{th} = 10dB$.

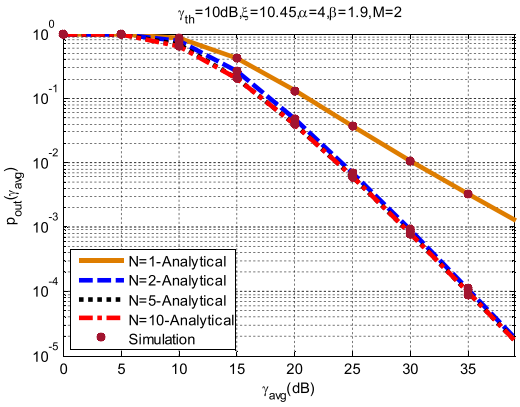

Fig. 7. Outage probability of the proposed structure as a function of average SNR for the different number of receive antennas, for moderate ($\alpha = 4$, $\beta = 1.9, \xi = 10.45$) regime of Gamma-Gamma atmospheric turbulence with the effect of pointing error, when the number of relays is $M = 2$ and $\gamma_{th} = 10dB$.

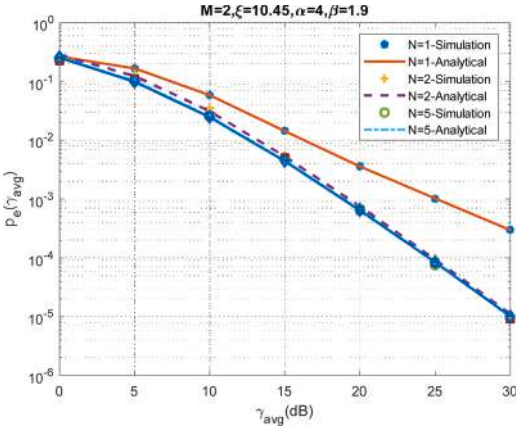

Fig. 8. Bit Error Rate of the proposed structure as a function of average SNR for different number of transmitter antennas, for moderate ($\alpha = 4, \beta = 1.9, \xi = 10.45$) regime of Gamma-Gamma atmospheric turbulence with the effect of pointing error, when number of relays is $M = 2$.

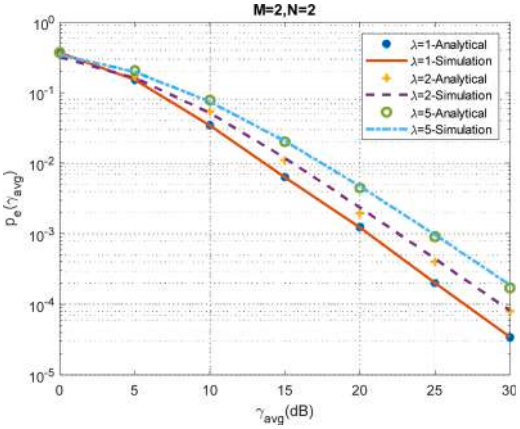

Fig. 9. Bit Error Rate of the proposed structure as a function of average SNR for various variances of Negative Exponential atmospheric turbulence, when number of receive antennas is $N = 2$ and number of relays is $M = 2$.

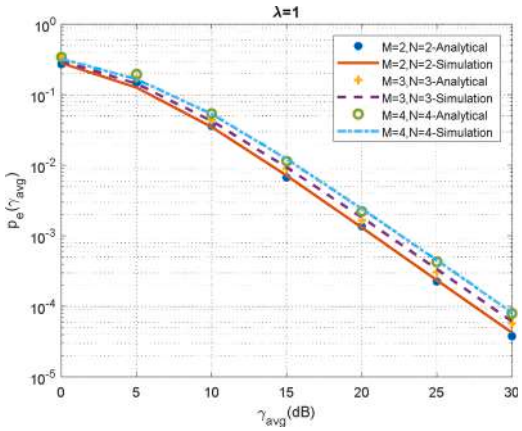

Fig. 10. Bit Error Rate of the proposed structure as a function of average SNR for different number of receive antennas and different number of relays, for Negative Exponential atmospheric turbulence with unit variance.

additional complexity and latency. The proposed structure was a bit more sensitive to Negative Exponential atmospheric turbulence than Gamma-Gamma atmospheric turbulence with the effect of pointing error. Hence the proposed structure is particularly suitable for urban communications which encounter frequent changes in atmospheric turbulence.

Declaration of Competing Interest

The authors report no declarations of interest.

Appendix A

Using [63], the pdf of Gamma-Gamma atmospheric turbulence with the effect of pointing error becomes as follows:

$$\begin{aligned} f_{\gamma_{FSO}}(\gamma) = {} & \frac{\xi^2\Gamma(\alpha-\xi^2)\Gamma(\beta-\xi^2)}{2\Gamma(\alpha)\Gamma(\beta)\gamma}\left(\alpha\beta\kappa\sqrt{\frac{\gamma}{\overline{\gamma}_{FSO}}}\right)^{\xi^2} \times {}_1F_2\left(0;1-\alpha+\xi^2,1-\beta+\xi^2;\alpha\beta\kappa\sqrt{\frac{\gamma}{\overline{\gamma}_{FSO}}}\right) \\ & + \frac{\xi^2\Gamma(\xi^2-\alpha)\Gamma(\beta-\alpha)}{2\Gamma(\alpha)\Gamma(\beta)\Gamma(\xi^2+1-\alpha)\gamma}\left(\alpha\beta\kappa\sqrt{\frac{\gamma}{\overline{\gamma}_{FSO}}}\right)^{\alpha} \times {}_1F_2\left(\alpha-\xi^2;1-\xi^2+\alpha,1-\beta+\alpha;\alpha\beta\kappa\sqrt{\frac{\gamma}{\overline{\gamma}_{FSO}}}\right) \\ & + \frac{\xi^2\Gamma(\alpha-\beta)\Gamma(\xi^2-\beta)}{2\Gamma(\alpha)\Gamma(\beta)\Gamma(\xi^2+1-\beta)\gamma}\left(\alpha\beta\kappa\sqrt{\frac{\gamma}{\overline{\gamma}_{FSO}}}\right)^{\beta} \times {}_1F_2\left(\beta-\xi^2;1-\xi^2+\beta,1-\alpha+\beta;\alpha\beta\kappa\sqrt{\frac{\gamma}{\overline{\gamma}_{FSO}}}\right) \end{aligned} \tag{24}$$

where ${}_pF_q\left(a_1,\ldots,a_p;b_1,\ldots,b_q;z\right)$ is the Hyper-Geometric function [63]. Using [63], the above expression becomes as follows:

$$\begin{aligned} f_{\gamma_{FSO}}(\gamma) = {} & \frac{\xi^2\Gamma(\alpha-\xi^2)\Gamma(\beta-\xi^2)}{2\Gamma(\alpha)\Gamma(\beta)}(\alpha\beta\kappa)^{\xi^2}\left(\frac{\gamma}{\overline{\gamma}_{FSO}}\right)^{\frac{\xi^2}{2}-1} + \sum_{n=0}^{\infty}\frac{\xi^2\Gamma(\beta-\alpha)(\alpha-\xi^2)_n}{2\Gamma(\alpha)\Gamma(\beta)(\xi^2-\alpha)(1-\xi^2+\alpha)_n(1-\beta+\alpha)_n n!}(\alpha\beta\kappa)^{n+\alpha}\left(\frac{\gamma}{\overline{\gamma}_{FSO}}\right)^{\frac{n+\alpha}{2}-1} \\ & + \sum_{n=0}^{\infty}\frac{\xi^2\Gamma(\alpha-\beta)(\beta-\xi^2)_n}{2\Gamma(\alpha)\Gamma(\beta)(\xi^2-\beta)(1-\xi^2+\beta)_n(1-\alpha+\beta)_n n!}(\alpha\beta\kappa)^{n+\beta}\left(\frac{\gamma}{\overline{\gamma}_{FSO}}\right)^{\frac{n+\beta}{2}-1}, \end{aligned} \tag{25}$$

where $()_n$ is the well-known pochhammer symbol. Integrating the above equation, CDF of Gamma-Gamma atmospheric turbulence with the effect of pointing error becomes as follows:

$$\begin{aligned} F_{\gamma_{FSO}}(\gamma) = {} & \frac{\Gamma(\alpha-\xi^2)\Gamma(\beta-\xi^2)}{\Gamma(\alpha)\Gamma(\beta)}(\alpha\beta\kappa)^{\xi^2}\left(\frac{\gamma}{\overline{\gamma}_{FSO}}\right)^{\frac{\xi^2}{2}} + \sum_{n=0}^{\infty}\frac{\xi^2\Gamma(\beta-\alpha)(\alpha-\xi^2)_n}{(n+\alpha)\Gamma(\alpha)\Gamma(\beta)(\xi^2-\alpha)(1-\xi^2+\alpha)_n(1-\beta+\alpha)_n n!}(\alpha\beta\kappa)^{n+\alpha} \times \left(\frac{\gamma}{\overline{\gamma}_{FSO}}\right)^{\frac{n+\alpha}{2}} \\ & + \sum_{n=0}^{\infty}\frac{\xi^2\Gamma(\xi^2-\beta)(\beta-\xi^2)_n}{(n+\beta)\Gamma(\alpha)\Gamma(\beta)(\alpha-\beta)(1-\xi^2+\beta)_n(1-\alpha+\beta)_n n!} \times (\alpha\beta\kappa)^{n+\beta}\left(\frac{\gamma}{\overline{\gamma}_{FSO}}\right)^{\frac{n+\beta}{2}} \\ = {} & X_0\left(\frac{\gamma}{\overline{\gamma}_{FSO}}\right)^{\frac{\xi^2}{2}} + \sum_{n=0}^{\infty}Y_n\left(\frac{\gamma}{\overline{\gamma}_{FSO}}\right)^{\frac{n+\alpha}{2}} + \sum_{n=0}^{\infty}Z_n\left(\frac{\gamma}{\overline{\gamma}_{FSO}}\right)^{\frac{n+\beta}{2}} \end{aligned} \tag{26}$$

Appendix B

From approximation [63], at $\gamma \gg 1$, the pdf of Gamma-Gamma atmospheric turbulence with the effect of pointing error becomes as follows:

$$f_\gamma(\gamma) \cong \begin{cases} \dfrac{\xi^2\Gamma(\alpha-\beta)}{2\Gamma(\alpha)\Gamma(\beta)(\xi^2-\beta)\gamma}\left(\alpha\beta\kappa\sqrt{\dfrac{\gamma}{\bar{\gamma}_{FSO}}}\right)^{\beta} & \xi^2 > \beta, \alpha > \beta \\ \dfrac{\xi^2\Gamma(\beta-\xi^2)\Gamma(\alpha-\xi^2)}{2\Gamma(\alpha)\Gamma(\beta)\gamma}\left(\alpha\beta\kappa\sqrt{\dfrac{\gamma}{\bar{\gamma}_{FSO}}}\right)^{\xi^2} & \alpha > \xi^2, \beta > \xi^2 \\ \dfrac{\xi^2\Gamma(\beta-\alpha)}{2\Gamma(\alpha)\Gamma(\beta)(\xi^2-\alpha)\gamma}\left(\alpha\beta\kappa\sqrt{\dfrac{\gamma}{\bar{\gamma}_{FSO}}}\right)^{\alpha} & \beta > \alpha, \xi^2 > \alpha \end{cases} \tag{24}$$

Integrating the above equation, CDF of Gamma-Gamma atmospheric turbulence with the effect of pointing error is as:

$$F_\gamma(\gamma) \cong \begin{cases} \dfrac{\xi^2\Gamma(\alpha-\beta)}{\Gamma(\alpha)\Gamma(\beta+1)(\xi^2-\beta)}\left(\alpha\beta\kappa\sqrt{\dfrac{1}{\bar{\gamma}_{FSO}}}\right)^{\beta}\gamma^{\frac{\beta}{2}} & \xi^2 > \beta, \alpha > \beta \\ \dfrac{\Gamma(\beta-\xi^2)\Gamma(\alpha-\xi^2)}{\Gamma(\alpha)\Gamma(\beta)}\left(\alpha\beta\kappa\sqrt{\dfrac{1}{\bar{\gamma}_{FSO}}}\right)^{\xi^2}\gamma^{\frac{\xi^2}{2}} & \alpha > \xi^2, \beta > \xi^2 \\ \dfrac{\xi^2\Gamma(\beta-\alpha)}{\Gamma(\alpha+1)\Gamma(\beta)(\xi^2-\alpha)}\left(\alpha\beta\kappa\sqrt{\dfrac{1}{\bar{\gamma}_{FSO}}}\right)^{\alpha}\gamma^{\frac{\alpha}{2}} & \beta > \alpha, \xi^2 > \alpha \end{cases} = \begin{cases} \varpi\gamma^{\frac{\beta}{2}} & (1) \\ \rho\gamma^{\frac{\xi^2}{2}} & (2) \\ \vartheta\gamma^{\frac{\alpha}{2}} & (3) \end{cases} \tag{27}$$

Appendix C. Supplementary data

Supplementary material related to this article can be found, in the online version, at doi:https://doi.org/10.1016/j.ijleo.2020.165883.

References

[1] M.T. Dabiri, S.M.S. Sadough, M.A. Khalighi, FSO channel estimation for OOK modulation with APD receiver over atmospheric turbulence and pointing errors, Opt. Commun. 402 (2017) 577–584.
[2] F.J. Lopez-Martinez, G. Gomez, J.M. Garrido-Balsells, Physical-layer security in free-space optical communications, IEEE Photonics J. 7 (2) (2015) 1–14.
[3] H. Kaushal, V.K. Jain, S. Ka, Free Space Optical Communication, Springer, India, 2017, p. 60.
[4] H.A. Fadhil, A. Amphawan, H.A. Shamsuddin, T.H. Abd, H.M. Al-Khafaji, S.A. Aljunid, N. Ahmed, Optimization of free space optics parameters: an optimum solution for bad weather conditions, Optik 124 (19) (2013) 3969–3973.
[5] P. Puri, P. Garg, M. Aggarwal, Analysis of spectrally efficient two-way relay assisted free space optical systems in atmospheric turbulence with path loss, Int. J. Commun. Syst. 29 (1) (2016) 99–112.
[6] W. Liu, W. Shi, J. Cao, Y. Lv, K. Yao, S. Wang, et al., Bit error rate analysis with real-time pointing errors correction in free space optical communication systems, Optik 125 (1) (2014) 324–328.
[7] M. Uysal, C. Capsoni, Z. Ghassemlooy, A. Boucouvalas, E. Udvary (Eds.), Optical Wireless Communications: an Emerging Technology, Springer, 2016.
[8] W. Gappmair, H.E. Nistazakis, Subcarrier PSK performance in terrestrial FSO links impaired by gamma-gamma fading, pointing errors, and phase noise, J. Light. Technol. 35 (9) (2017) 1624–1632.
[9] P.K. Sharma, A. Bansal, P. Garg, T. Tsiftsis, R. Barrios, Relayed FSO communication with aperture averaging receivers and misalignment errors, Iet Commun. 11 (1) (2017) 45–52.
[10] M.A. Amirabadi, V.T. Vakili, A new optimization problem in FSO communication system, Ieee Commun. Lett. 22 (7) (2018) 1442–1445.
[11] T. Rakia, H.C. Yang, M.S. Alouini, F. Gebali, Outage analysis of practical FSO/RF hybrid system with adaptive combining, Ieee Commun. Lett. 19 (8) (2015) 1366–1369.
[12] L. Chen, W. Wang, C. Zhang, Multiuser diversity over parallel and hybrid FSO/RF links and its performance analysis, IEEE Photonics J. 8 (3) (2016) 1–9.
[13] V.V. Mai, A.T. Pham, Adaptive multi-rate designs for hybrid fso/rf systems over fading channels, December, in: 2014 IEEE Globecom Workshops (GC Wkshps), IEEE, 2014, pp. 469–474.
[14] Z. Kolka, Z. Kincl, V. Biolkova, D. Biolek, Hybrid FSO/RF test link, October, in: 2012 IV International Congress on Ultra Modern Telecommunications and Control Systems, IEEE, 2012, pp. 502–505.
[15] A. AbdulHussein, A. Oka, T.T. Nguyen, L. Lampe, Rateless coding for hybrid free-space optical and radio-frequency communication, Ieee Trans. Wirel. Commun. 9 (3) (2010) 907–913.
[16] W. Zhang, S. Hranilovic, C. Shi, Soft-switching hybrid FSO/RF links using short-length raptor codes: design and implementation, Ieee J. Sel. Areas Commun. 27 (9) (2009) 1698–1708.
[17] B. Makki, T. Svensson, M. Brandt-Pearce, M.S. Alouini, Performance analysis of RF-FSO multi-hop networks, March, in: 2017 IEEE Wireless Communications and Networking Conference (WCNC), IEEE, 2017, pp. 1–6.
[18] M.A. Amirabadi, V.T. Vakili, A novel hybrid FSO/RF communication system with receive diversity, Optik 184 (2019) 293–298.
[19] M.A. Amirabadi, An Optimization Problem on the Performance of FSO Communication System, arXiv preprint arXiv:1902.10043, 2019.
[20] B. Makki, T. Svensson, T. Eriksson, M.S. Alouini, On the performance of RF-FSO links with and without hybrid ARQ, Ieee Trans. Wirel. Commun. 15 (7) (2016) 4928–4943.

[21] T. Rakia, H.C. Yang, F. Gebali, M.S. Alouini, Power adaptation based on truncated channel inversion for hybrid FSO/RF transmission with adaptive combining, IEEE Photonics J. 7 (4) (2015) 1–12.
[22] E. Soleimani-Nasab, M. Uysal, Generalized performance analysis of mixed RF/FSO cooperative systems, Ieee Trans. Wirel. Commun. 15 (1) (2015) 714–727.
[23] K. Kumar, D.K. Borah, Quantize and encode relaying through FSO and hybrid FSO/RF links, Ieee Trans. Veh. Technol. 64 (6) (2014) 2361–2374.
[24] R. Boluda-Ruiz, A. García-Zambrana, B. Castillo-Vázquez, C. Castillo-Vázquez, MISO relay-assisted FSO systems over gamma–gamma fading channels with pointing errors, Ieee Photonics Technol. Lett. 28 (3) (2015) 229–232.
[25] R. Boluda-Ruiz, A. García-Zambrana, B. Castillo-Vázquez, C. Castillo-Vázquez, Ergodic capacity analysis of decode-and-forward relay-assisted FSO systems over alpha–Mu fading channels considering pointing errors, IEEE Photonics J. 8 (1) (2015) 1–11.
[26] S. Anees, M.R. Bhatnagar, Performance of an amplify-and-forward dual-hop asymmetric RF–FSO communication system, J. Opt. Commun. Netw. 7 (2) (2015) 124–135.
[27] J. Zhang, L. Dai, Y. Zhang, Z. Wang, Unified performance analysis of mixed radio frequency/free-space optical dual-hop transmission systems, J. Light. Technol. 33 (11) (2015) 2286–2293.
[28] Z. Jing, Z. Shang-hong, Z. Wei-hu, C. Ke-fan, Performance analysis for mixed FSO/RF Nakagami-m and Exponentiated Weibull dual-hop airborne systems, Opt. Commun. 392 (2017) 294–299.
[29] E. Zedini, I.S. Ansari, M.S. Alouini, Performance analysis of mixed Nakagami-$ m $ and Gamma–Gamma dual-hop FSO transmission systems, IEEE Photonics J. 7 (1) (2014) 1–20.
[30] M.A. Amirabadi, V.T. Vakili, Performance Analysis of Hybrid FSO/RF Communication Systems with Alamouti Coding or Antenna Selection, arXiv preprint arXiv:1802.07286, 2018.
[31] L. Kong, W. Xu, L. Hanzo, H. Zhang, C. Zhao, Performance of a free-space-optical relay-assisted hybrid RF/FSO system in generalized $ M $-distributed channels, IEEE Photonics J. 7 (5) (2015) 1–19.
[32] V. Jamali, D.S. Michalopoulos, M. Uysal, R. Schober, Mixed RF and hybrid RF/FSO relaying, December, in: 2015 IEEE Globecom Workshops (GC Wkshps), IEEE, 2015, pp. 1–6.
[33] G.T. Djordjevic, M.I. Petkovic, A.M. Cvetkovic, G.K. Karagiannidis, Mixed RF/FSO relaying with outdated channel state information, IEEE J. Sel. Areas Commun. 33 (9) (2015) 1935–1948.
[34] N.I. Miridakis, M. Matthaiou, G.K. Karagiannidis, Multiuser relaying over mixed RF/FSO links, IEEE Trans. Commun. 62 (5) (2014) 1634–1645.
[35] E. Zedini, H. Soury, M.S. Alouini, On the performance analysis of dual-hop mixed FSO/RF systems, IEEE Trans. Wirel. Commun. 15 (5) (2016) 3679–3689.
[36] E. Zedini, H. Soury, M.S. Alouini, On the performance of dual-hop FSO/RF systems, August, in: 2015 International Symposium on Wireless Communication Systems (ISWCS), IEEE, 2015, pp. 31–35.
[37] E. Lee, J. Park, D. Han, G. Yoon, Performance analysis of the asymmetric dual-hop relay transmission with mixed RF/FSO links, IEEE Photonics Technol. Lett. 23 (21) (2011) 1642–1644.
[38] H. Samimi, M. Uysal, End-to-end performance of mixed RF/FSO transmission systems, IEEE/OSA J. Opt. Commun. Network. 5 (11) (2013) 1139–1144.
[39] B. Bag, A. Das, A. Chandra, C. Bose, Capacity analysis for Rayleigh/gamma-gamma mixed RF/FSO link with fixed-gain AF relay, IEICE Trans. Commun. 100 (10) (2017) 1747–1757.
[40] E. Zedini, H. Soury, M.S. Alouini, Dual-hop FSO transmission systems over gamma–gamma turbulence with pointing errors, IEEE Trans. Wirel. Commun. 16 (2) (2016) 784–796.
[41] N. Varshney, P. Puri, Performance analysis of decode-and-forward-based mixed MIMO-RF/FSO cooperative systems with source mobility and imperfect CSI, J. Light. Technol. 35 (11) (2017) 2070–2077.
[42] P.K. Sharma, A. Bansal, P. Garg, Relay assisted bi-directional communication in generalized turbulence fading, J. Light. Technol. 33 (1) (2014) 133–139.
[43] P.K. Sharma, P. Garg, Bi-directional decode-XOR-forward relaying over\(\mathcal {m}\)-distributed free space optical links, Ieee Photonics Technol. Lett. 26 (19) (2014) 1916–1919.
[44] B. Ashrafzadeh, E. Soleimani-Nasab, M. Kamandar, M. Uysal, A framework on the performance analysis of dual-hop mixed FSO-RF cooperative systems, IEEE Trans. Commun. 67 (7) (2019) 4939–4954.
[45] I. Trigui, S. Affes, A.M. Salhab, M.S. Alouini, Multi-user mixed FSO-RF systems with aperture selection under poisson field interference, IEEE Access 7 (2019) 73764–73781.
[46] H. Arezumand, H. Zamiri-Jafarian, E. Soleimani-Nasab, Outage and diversity analysis of underlay cognitive mixed RF-FSO cooperative systems, J. Opt. Commun. Netw. 9 (10) (2017) 909–920.
[47] M.A. Amirabadi, V.T. Vakili, Performance of a relay-assisted hybrid FSO/RF communication system, Phys. Commun. 35 (2019), 100729.
[48] M.A. Amirabadi, Performance Analysis of a Novel Hybrid FSO/RF Communication System, arXiv preprint arXiv:1802.07160, 2018.
[49] I.S. Ansari, M.S. Alouini, F. Yilmaz, On the performance of hybrid RF and RF/FSO fixed gain dual-hop transmission systems, April, in: 2013 Saudi International Electronics, Communications and Photonics Conference, IEEE, 2013, pp. 1–6.
[50] H. Saidi, K. Tourki, N. Hamdi, Performance analysis of PSK modulation in DF dual-hop hybrid RF/FSO system over gamma gamma channel, November, in: 2016 International Symposium on Signal, Image, Video and Communications (ISIVC), IEEE, 2016, pp. 213–216.
[51] P. Wang, T. Cao, L. Guo, R. Wang, Y. Yang, Performance analysis of multihop parallel free-space optical systems over exponentiated Weibull fading channels, IEEE Photonics J. 7 (1) (2015) 1–17.
[52] M.A. Kashani, M. Uysal, Outage performance of FSO multi-hop parallel relaying, April, 2012 20th Signal Processing and Communications Applications Conference (SIU) (2012) 1–4. IEEE.
[53] M.A. Kashani, M. Uysal, Outage performance and diversity gain analysis of free-space optical multi-hop parallel relaying, J. Opt. Commun. Netw. 5 (8) (2013) 901–909.
[54] M.A. Amirabadi, V.T. Vakili, Performance comparison of two novel relay-assisted hybrid FSO/RF communication systems, Iet Commun. 13 (11) (2019) 1551–1556.
[55] H. Arezumand, H. Zamiri-Jafarian, E. Soleimani-Nasab, Exact and asymptotic analysis of partial relay selection for cognitive RF-FSO systems with non-zero boresight pointing errors, IEEE Access 7 (2019) 58611–58625.
[56] T.A. Tsiftsis, H.G. Sandalidis, G.K. Karagiannidis, N.C. Sagias, Multihop free-space optical communications over strong turbulence channels, June, in: IEEE2006 IEEE International Conference on Communications, Vol. 6, 2006, pp. 2755–2759.
[57] G. Farhadi, N.C. Beaulieu, Capacity of amplify-and-forward multi-hop relaying systems under adaptive transmission, Ieee Trans. Commun. 58 (3) (2010) 758–763.
[58] M. Najafi, V. Jamali, R. Schober, Optimal relay selection for the parallel hybrid RF/FSO relay channel: non-buffer-aided and buffer-aided designs, I$ Trans. Commun. 65 (7) (2017) 2794–2810.
[59] H. Kazemi, M. Uysal, F. Touati, H. Haas, Outage performance of multi-hop hybrid FSO/RF communication systems, September, in: 2015 4th International Workshop on Optical Wireless Communications (IWOW), IEEE, 2015, pp. 83–87.
[60] B. Makki, T. Svensson, M. Brandt-Pearce, M.S. Alouini, On the performance of millimeter wave-based RF-FSO multi-hop and mesh networks, IEEE Trans. Wirel. Commun. 16 (12) (2017) 7746–7759.
[61] D.H. Ai, D.T. Quang, N.N. Nam, H.D. Trung, N.X. Dung, Capacity analysis of amplify-and-forward free-space optical communication systems over atmospheric turbulence channels, April, in: 2017 Seventh International Conference on Information Science and Technology (ICIST), IEEE, 2017, pp. 103–108.
[62] H. Saidi, K. Tourki, N. Hamdi, Performance analysis of PSK modulation in DF dual-hop hybrid RF/FSO system over gamma gamma channel, November, in: 2016 International Symposium on Signal, Image, Video and Communications (ISIVC), IEEE, 2016, pp. 213–216.

[63] N.I. Miridakis, T.A. Tsiftsis, EGC reception for FSO systems under mixture-Gamma fading channels and pointing errors, IEEE Commun. Lett. 21 (6) (2017) 1441–1444.
[64] M.R. Bhatnagar, Z. Ghassemlooy, Performance analysis of gamma–gamma fading FSO MIMO links with pointing errors, J. Light. Technol. 34 (9) (2016) 2158–2169.
[65] Mathworld, W. (2009). Online]: http://functions.wolfram.com/HypergeometricFunctions.